Crystal Structure of Bis(2,2'-bipyridyl)monochlorocopper(II) Tetrafluoroborate. A Relook at the Structural Pathway of the Bis(2,2'- bipyridyl)monochlorocopper(II) Cation†

Patrick Nagle, Edward O'Sullivan, and Brian J. Hathaway*
The Chemistry Department, University College, Cork, Ireland
Edgar Muller
Dep. de Chimie Minerale, Analytique et Appliquee, Universite de Geneve, 30 quai Ernest Ansermet, 1211 Geneve 4, Switzerland

The crystal structure of $[Cu(bipy)_2Cl]BF_4$ (**I**) (bipy = 2,2'-bipyridyl) has been determined using diffractometer data collection. It was solved by the heavy-atom method and successive Fourier difference syntheses. Compound (**I**) crystallises in the monoclinic space group $P2_1/n$ with a = 16.187(4), b = 12.177(3), c = 10.793(3) Å, β = 104.49(3)°, Z = 4, and R = 0.058 for 1 451 unique reflections. The CuN_4Cl chromophore involves a square-based-pyramidal distorted trigonal-bipyramidal stereochemistry. The extent of the square-pyramidal distortion is mirrored in the twin-peaked electronic reflectance spectrum, with absorption maxima at 10 100 and 13 900 cm^{-1}. The structure of complex (**I**) is compared with those of a series of eight cation distortion isomers of $[Cu(bipy)_2Cl]Y$ which are related by a structural pathway. The nine complexes have been subjected to scatter-plot and factor-group analysis and the feasibility of extending the structural pathway to include two $[Cu(bipy)_2Br]^+$ and two $[Cu(bipy)_2I]^+$ complexes is examined.

One of the consequences of the Jahn–Teller theorem[1] in the stereochemistry of the copper(II) ion has been termed the plasticity effect,[2] and suggests that the various distortion isomers of the copper(II) ion are related by soft modes of vibration of the more regular stereochemistries.[3] Using the cation and anion distortion isomers that are available, the cations[4,5] $[Cu(bipy)_2Cl]^+$ (bipy = 2,2'-bipyridyl) or $[Cu(dien)(bipyam)]^{2+}$ (dien = diethylenetriamine, bipyam = di-2-pyridylamine) or the anions[6,7] $[CuCl_4]^{2-}$ or $[Cu(NO_2)_6]^{4-}$, attempts have been made to determine the modes of vibration that establish the direction of the structural pathways connecting the extreme stereochemistries involved, Figure 1. However, even in the case of cation or anion distortion isomers, the number of comparable structures may not be enough to justify the suggestion of a structural pathway. In the case of $[Cu(dien)(bipyam)]^{2+}$ (ref. 5) only three structures were involved, while with $[Cu(bipy)_2Cl]^+$ (ref. 4) five structures were used. In both cases it was suggested that the individual local molecular structures lay along a structural pathway from a trigonal-bipyramidal to a square-based-pyramidal distorted trigonal-bipyramidal geometry. These structural changes were also correlated with changes in the electronic reflectance spectra.[4–6] Recently[8] the effect of pressure on the electronic spectra of the $[Cu(dien)(bipyam)]^{2+}$ and $[Cu(bipy)_2Cl]^+$ distortion isomers has suggested that, with increasing pressure, the structures appear to follow the direction of the structural pathway proposed earlier.[5] This suggests that the concept of a structural pathway may be of importance in the solid state in determining the way that species change their structure, with change of pressure. Since the original publication of the five cation distortion isomers of $[Cu(bipy)_2Cl]^+$ three more structures have been reported[9–11] and with the present structure, $[Cu(bipy)_2Cl]BF_4$, this increases the total number of $[Cu(bipy)_2Cl]^+$ cation distortion isomers to nine. Using this increased data base the original scatter plots have been re-examined and the data analysis extended to the use of factor group analysis[12] using the FACAN program.[13,14]

Experimental

The complex $[Cu(bipy)_2Cl]BF_4$ (**I**) was prepared by adding a boiling solution of bipy (0.4 g, 2.56 mmol) in absolute alcohol (30 cm^3) to a boiling solution of $Cu(BF_4)_2 \cdot 6H_2O$ (0.44 g, 1.28 mmol), $NH_2OH \cdot HCl$ (0.2 g, 2.87 mmol) and 0.88NH_4OH (1 cm^3) in water (30 cm^3). The resulting reddish brown copper(I) solution was allowed to oxidise in air[15,16] and yielded an initial precipitate of blue crystals which analysed as $[Cu(bipy)_2(NH_3)][BF_4]_2$.[17] The mother-liquor was allowed to evaporate further to yield green crystals of complex (**I**). The crystals were filtered off, washed with the mother-liquor, and dried at the pump (Found: C, 48.10; H, 3.10; N, 11.60. Calc. for $C_{20}H_{16}BClCuF_4N_4$: C, 48.20; H, 3.20; N, 11.25%).

Crystallography.—Crystal data. $C_{20}H_{16}BClCuF_4N_4$, M = 496.15, monoclinic, space group $P2_1/n$, a = 16.187(4), b = 12.177(3), c = 10.793(3) Å, β = 104.49(3)°, U = 2 059.73 Å^3, D_m = 1.58 g cm^{-3}, D_c = 1.61 g cm^{-3}, Z = 4, $F(000)$ = 996, Mo-K_α radiation, λ = 0.710 69 Å, μ(Mo-K_α) = 11.84 cm^{-1}.

The unit-cell dimensions were determined (25 reflections, θ 3—25°) and the intensities collected on a Phillips PW1100 four-circle diffractometer with graphite-monochromatised Mo-K_α radiation. Reflections with $3.0 < \theta < 25°$ in one quadrant were examined in the θ—2θ scan mode, with a constant scan speed of 0.05° s^{-1}, and a variable scan width of (0.7 + 0.1 tan θ)°. 1 719 Reflections were collected [$I > 2.5\sigma(I)$], h −18 to 18, k 0—12, l 0—12, and 1 451 unique reflections were retained. Lorentz and polarisation corrections were applied (DRED), but no correction was made for the absorption. The structure was solved by the SHELX 76[18] and SHELX 86[19] direct methods, Fourier difference techniques, and refined by block-matrix least-squares analysis, $\Sigma w(|F_o| - |F_c|)^2$, with initial $w = 1/\sigma^2(F_o)$, and then with anisotropic thermal parameters for all the non-H atoms,

† *Supplementary data available* (No. SUP 56782, 6 pp.): scatter plots. See Instructions for Authors, *J. Chem. Soc., Dalton Trans.*, 1990, Issue 1, pp. xix—xxii.

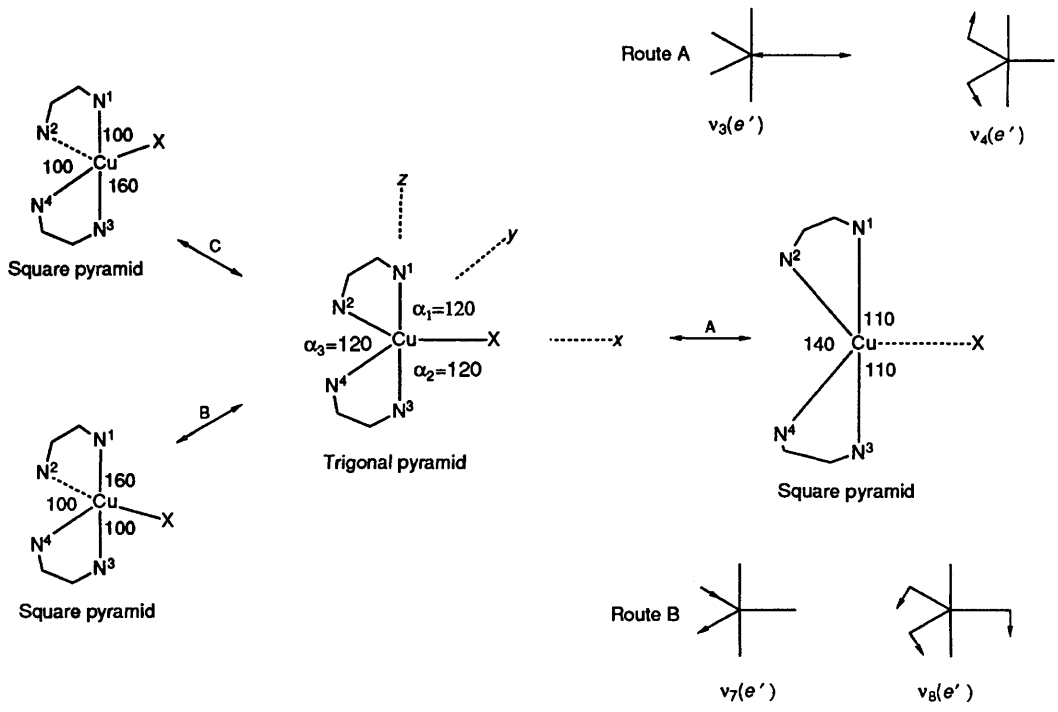

Figure 1. Structural pathways (angles in °) for the distortion of the CuN_4Cl chromophore of the $[Cu(bipy)_2Cl]^+$ cation from trigonal bipyramidal to square-based pyramidal, involving the routes A—C

Table 1. Fractional atomic co-ordinates with estimated standard deviations (e.s.d.s) in parentheses for $[Cu(bipy)_2Cl]BF_4$

Atom	*x*	*y*	*z*	Atom	*x*	*y*	*z*
Cu	−0.136 24(7)	0.544 38(11)	0.736 10(12)	C(12)	−0.392 2(8)	0.488 2(10)	0.752 1(13)
Cl	−0.136 8(2)	0.356 9(3)	0.726 9(4)	C(13)	−0.395 7(6)	0.542 6(12)	0.861 3(12)
N(1)	−0.022 6(5)	0.555 8(7)	0.694 2(8)	C(14)	−0.326 3(7)	0.601 6(10)	0.928 3(11)
C(1)	0.043 7(7)	0.492 8(10)	0.747 3(11)	C(15)	−0.253 5(6)	0.601 4(8)	0.882 6(10)
C(2)	0.117 6(6)	0.496 4(11)	0.709 0(13)	N(4)	−0.107 9(5)	0.645 6(7)	0.903 7(7)
C(3)	0.124 5(7)	0.570 5(11)	0.613 2(13)	C(16)	−0.177 1(6)	0.665 0(8)	0.947 1(10)
C(4)	0.055 4(8)	0.635 5(9)	0.559 4(12)	C(17)	−0.175 1(7)	0.739 3(10)	1.043 0(11)
C(5)	−0.018 5(5)	0.628 7(8)	0.601 9(10)	C(18)	−0.098 8(10)	0.798 5(11)	1.092 1(11)
N(2)	−0.161 5(5)	0.669 7(7)	0.601 0(7)	C(19)	−0.030 3(8)	0.780 0(11)	1.046 2(11)
C(6)	−0.094 2(6)	0.694 7(7)	0.553 1(9)	C(20)	−0.037 0(7)	0.702 8(10)	0.951 8(12)
C(7)	−0.101 0(8)	0.777 8(11)	0.464 0(14)	B	−0.131 9(9)	1.105 2(12)	1.229 7(15)
C(8)	−0.174 2(11)	0.835 0(11)	0.427 2(12)	F(1)	−0.081 2(5)	1.048 8(9)	1.326 0(9)
C(9)	−0.244 4(9)	0.811 6(11)	0.476 7(13)	F(2)	−0.192 1(5)	1.164 3(7)	1.269 2(8)
C(10)	−0.233 6(8)	0.730 3(11)	0.563 8(12)	F(3)	−0.180 3(8)	1.029 4(9)	1.150 3(13)
N(3)	−0.248 9(5)	0.546 6(7)	0.777 3(7)	F(4)	−0.089 0(5)	1.167 0(9)	1.167 5(10)
C(11)	−0.318 0(7)	0.490 0(10)	0.713 2(12)				

total 329 parameters. The positions of the hydrogen atoms were located from the difference map, when all the non-H atoms had been refined with anisotropic thermal parameters. The refinement converged when the maximum shift-to-error ratio of any parameter was less than 0.07 for the non-hydrogen atoms, with a refined weighting scheme $w = k/[\sigma(F_o) + g(F_o)^2]^{-1}$ and the final values of k and g were 0.5410 and 0.006 38, respectively. The final R and R' values were 0.058 and 0.061, respectively, and the maximum and minimum residual electron densities were 0.50 and −1.05 e Å^{-3}, respectively. Complex atom scattering factors were employed and those for Cu and Cl were corrected for anomalous dispersion.[20] All calculations were carried out with SHELX 76,[18] SHELX 86,[19] XANADU,[21] CHEM-X,[22] and PUBTAB[23] on the University College Cork mainframe IBM 4341 and VAX 11/780 computers. Final atomic co-ordinates are given in Table 1, selected bond lengths and angles in Table 2, and some mean plane data in Table 3. Figure 2

Table 2. Selected bond lengths (Å) and angles (°) of complex (**I**) with e.s.d.s in parentheses

Cu–Cl	2.285(3)	B–F(1)	1.341(15)
Cu–N(1)	2.006(7)	B–F(2)	1.363(14)
Cu–N(3)	1.983(7)	B–F(3)	1.365(15)
Cu–N(2)	2.079(8)	B–F(4)	1.316(14)
Cu–N(4)	2.142(8)		
N(2)–Cu–Cl (α_1)	134.8(3)	N(3)–Cu–N(2) (α_9)	97.8(3)
N(4)–Cu–Cl (α_2)	127.6(3)	N(4)–Cu–N(1) (α_{10})	96.7(3)
N(4)–Cu–N(2) (α_3)	97.6(3)	F(1)–B–F(2)	112(1)
N(1)–Cu–Cl (α_4)	93.1(3)	F(1)–B–F(3)	106(1)
N(3)–Cu–Cl (α_5)	91.7(3)	F(1)–B–F(4)	113(1)
N(2)–Cu–N(1) (α_6)	79.7(3)	F(2)–B–F(3)	102(1)
N(4)–Cu–N(3) (α_7)	79.5(3)	F(2)–B–F(4)	111(1)
N(3)–Cu–N(1) (α_8)	175.2(4)	F(3)–B–F(4)	111(1)

Table 3. Equations of the least-squares planes of complex (I) in the form $lX + mY + nZ = p$, where X, Y, and Z are orthogonal axes, with root mean square deviations (Å) in parentheses and deviations (Å) of relevant atoms from the planes in square brackets

Plane	l	m	n	p
(1) N(1), C(1)—C(5) (r.m.s.d. 0.0052)	2.9218	8.5414	6.7175	9.3520
(2) C(6)—C(10), N(2) (r.m.s.d. 0.0087) [N(2) −0.0141, C(10) 0.0132]	2.5456	7.9574	7.3126	9.3258
(3) N(1), C(1)—C(10), N(2) (r.m.s.d. 0.0356) [C(1) 0.0634, C(4) −0.0558, N(2) −0.0541]	2.6401	8.2467	7.0568	9.3905
(4) N(3), C(11)—C(15) (r.m.s.d. 0.0073) [C(12) −0.0125]	3.2092	−9.8785	5.2127	−2.1490
(5) C(16)—C(20), N(4) (r.m.s.d. 0.0074) [C(16) −0.0126]	2.1864	−8.6424	6.8601	0.3754
(6) N(3), C(11)—C(20), N(4) (r.m.s.d. 0.0873) [C(11) −0.1338, C(14) 0.1279, C(18) −0.1257)]	2.5024	−9.2951	6.1369	−0.8385

Angles (°) between planes: 1 and 2, 4.23; 4 and 5, 10.62; 3 and 6, 92.39.

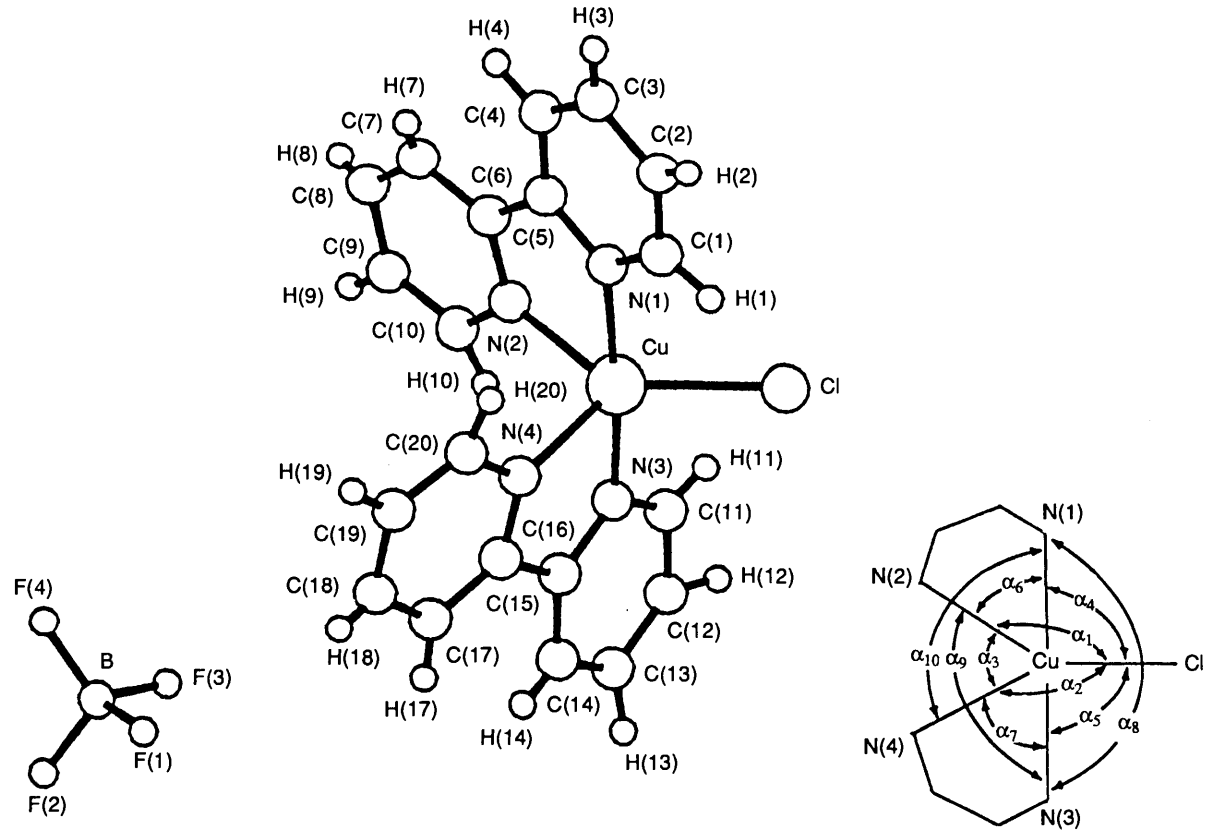

Figure 2. Molecular structure of $[Cu(bipy)_2Cl]BF_4$, showing the atom numbering scheme and angle notation for the CuN_4Cl chromophore

illustrates the molecular structure of complex (I), the atomic numbering scheme used, and the α_n angle notation. Figure 3 shows the crystal packing viewed down the c axis.

Additional material available from the Cambridge Crystallographic Data Centre comprises H-atom co-ordinates, thermal parameters and remaining bond lengths and angles.

Results and Discussion

The asymmetric unit of complex (I) involves a $[Cu(bipy)_2Cl]^+$ cation and a BF_4^- anion. The structure of the cation consists of a five-co-ordinate CuN_4Cl chromophore with a distorted trigonal-bipyramidal geometry. The out-of-plane bond lengths Cu–N(1) and Cu–N(3) are just significantly different, 2.006(7) and 1.983(7) Å, respectively [mean 1.995(7) Å], and are significantly shorter than the two in-plane distances Cu–N(2) and Cu–N(4), 2.079(8) and 2.142(8) Å, respectively [mean 2.111(8) Å]. The difference between the mean values (0.116 Å) is comparable with that (0.1 Å) previously reported for a trigonal-bipyramidal copper(II) stereochemistry.[24] The two in-plane Cu–N distances are themselves significantly different (0.063 Å). The chloride ion co-ordinates in-the-plane at a distance of 2.285(3) Å. The N(1)–Cu–N(3) angle of 175.2° is almost linear, with N(1)–Cu–Cl and N(3)–Cu–Cl 93.1 and 91.7°, respectively, *i.e.* greater than 90°, resulting in both the N(1) and N(3) atoms being bent away from the Cu–Cl bond. The in-plane angles distort significantly from the 120° of a regular trigonal-bipyramidal stereochemistry, with $\alpha_1 = 134.8(3)$, $\alpha_2 = 127.6(3)$, and $\alpha_3 = 97.6(3)°$, see Figure 2 (insert) for the angle notation used. The large α_1 angle lies opposite the longest in-plane Cu–N(4) distance of 2.142(8) Å and the sense of this distortion involves a square-based pyramidal distortion of the regular trigonal-bipyramidal CuN_4Cl chromophore,[4] route B (or C), Figure 1, with an elongation of the Cu–N(4) direction and α_1

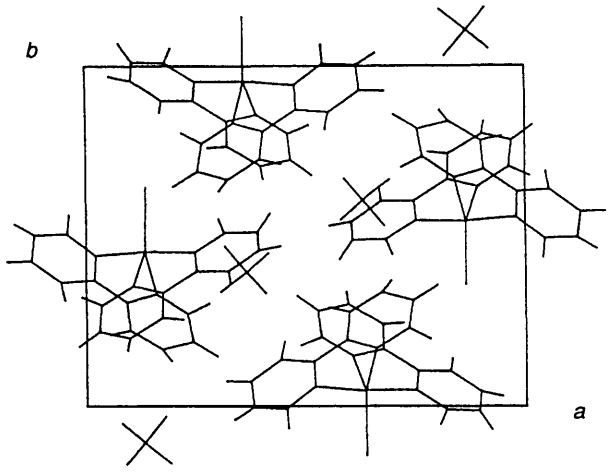

Figure 3. Packing of $[Cu(bipy)_2Cl]BF_4$ in the unit cell viewed down the approximate *c* axis

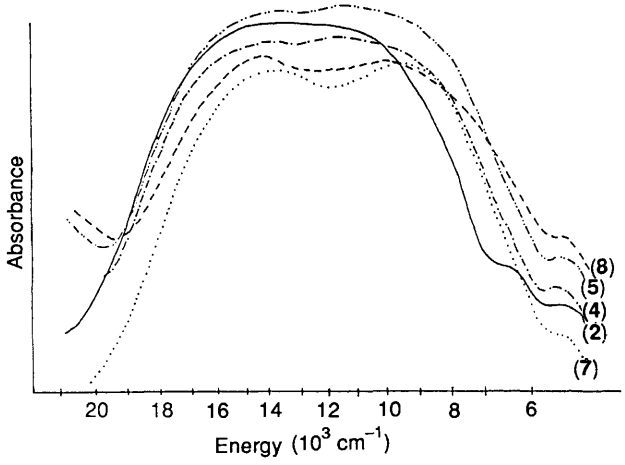

Figure 4. Electronic reflectance spectra of some $[Cu(bipy)_2X]Y$ complexes; see Table 4 for the notation used

representing the large basal angle. Using the notation of the insert to Figure 2, the magnitude of this square-based pyramidal distortion[25,26] can be measured by the τ value, *i.e.* $(\alpha_8 - \alpha_1)/60$, and which for (**I**) is 0.67. As the regular trigonal bipyramid and square-based pyramid have τ values of 1.00 and 0.00, respectively, the structure of (**I**) is best described as trigonal bipyramidal, with a significant square-pyramidal distortion. The bites of the bipy ligands are not significantly different, 79.7(3) and 79.5(3)° for the N(1)/N(2) and the N(3)/N(4) ligands, respectively. The individual pyridine rings of the chelates are reasonably planar, Table 3, with root-mean-square deviations less than 0.0087 Å and involving angles of twist of 4.23 and 10.62° for the N(1)/N(2) and the N(3)/N(4) ligands, respectively. The full mean planes of the bipy ligands are inclined to each other at 92.39°.

The structure of the present complex is a further example of a cation distortion isomer of $[Cu(bipy)_2Cl]Y$, which have been used to suggest a structural pathway for the square-based pyramidal distortion of a regular trigonal-bipyramidal CuN_4Cl chromophore.[4] Table 4(*a*) lists the relevant bond lengths and angles of the complexes of known crystal structure, in order of decreasing τ value. In order to place (**I**), correctly, in this sequence of distortion along the structural pathway, from this point on in this paper it will be referred to as (**7**). These structures range from the almost regular trigonal-bipyramidal stereochemistries (τ = 1.0) of (**1**)—(**3**), through the intermediate distorted structures (τ = 0.80) of (**4**) and (**5**) to the marked square-pyramidal distortions (τ = 0.60) of (**7**)—(**9**).

The sense of the distortion in the present complex is characteristic of the CuN_4Cl chromophores of the remaining complexes in the series (**1**)—(**9**). As the Cu–N(4) bond elongates the α_1 angle opposite this bond increases (route B of the structural pathway in Figure 1), and reflects the structural trend of these CuN_4Cl chromophores. The extent of the distortion present in (**7**) may be determined by reference to the CuN_4Cl chromophores of the $[Cu(bipy)_2Cl]Y$ structures, Table 4(*a*), in particular to the bond length and angle distortions outlined above. The α_1 and α_2 angles of 134.8 and 127.6° in (**7**) show quite a significant deviation from 120°. The $\Delta\alpha_{1,2}$ value of 7.2° is significantly less than the extreme value of 24.3° present in (**9**) and is in fact similar to that found in the intermediate square-pyramidal distorted structures of (**4**) and (**5**). The α_3 angle of 97.6° in (**7**) is comparable to the lowest value in the series of 96.5° for (**8**). The in-plane bond-length distortion in the present complex, $\Delta N_{4,2} = 0.063$ Å, is the largest value observed in this series of distortion isomers, comparable to the extreme square-pyramidal distorted trigonal-bipyramidal geometries of (**8**) and (**9**). Thus, while the in-plane angular distortion of the present complex indicates an intermediate square-based pyramidal distortion of the CuN_4Cl chromophore, the extent of the in-plane bond length distortion and, in particular, the $\Delta N_{4,2}$ value, points to an extreme square-based pyramidal distortion. A similar conclusion can be drawn from the τ value of 0.67 for (**7**). The structural characteristics indicate that (**7**) represents one of the more extreme cases of square-pyramidal distortion in the $[Cu(bipy)_2Cl]^+$ cation distortion isomers. The structure most similar to it is that of (**8**).

E.S.R. Spectrum.—The e.s.r. spectrum of complex (**7**) is axial, $g_{\|} = 2.20$ and $g_{\perp} = 2.01$, consistent with a d_{z^2} ground state for the approximately trigonal-bipyramidal stereochemistry[4] of the CuN_4Cl chromophore present, $g_{\|} \gg g_{\perp} \approx 2.0$.

Electronic Spectra.—The electronic spectrum of complex (**7**), Figure 4 (Table 5), shows two peaks of similar intensity with absorption maxima at 10 100 and 13 900 cm^{-1}. The separation between the peaks of 3 800 cm^{-1} is comparable to the separation in (**8**) and reflects the similar extent of square-based pyramidal distortion present in the two complexes. The electronic spectra of the $[Cu(bipy)_2Cl]Y$ cation distortion isomers have been used to suggest an 'electronic criteria of stereochemistry' for the CuN_4Cl chromophore.[4] The regular trigonal-bipyramidal structure of (**3**) shows a single-peaked spectrum with an absorption maximum at 12 500 cm^{-1}. The intermediate square-based pyramidal distorted structures of (**4**) and (**5**) show broad single-peaked spectra with asymmetry to high energy. The extreme square-based pyramidal distortion present in (**8**) yields a double-peaked spectrum, with the lower-energy peak at 10 000 cm^{-1} and a separation of *ca.* 4 000 cm^{-1} between the peaks. These spectra are shown in Figure 4.

Scatter Plots.—The nine $[Cu(bipy)_2Cl]Y$ data sets of Table 4(*a*) currently represent the most extensive set of bond length and angle data for a related series of cation distortion isomers. As the original data set used to establish the structural pathway of Figure 1 only involved five structures,[4] the nine data sets have been used to prepare the scatter plots (see SUP 56782). As the τ value has been shown to be the most useful parameter to reflect the distortions of the CuN_4Cl chromophore,[25] Figure 5(*a*)—(*d*) displays the four most representative of these scatter plots, including τ. In the case of complex (**9**) there is no obvious reason for the 'erratic' behaviour of the data points.

The plots clearly confirm the general variation of the bond lengths and angles of the $[Cu(bipy)_2Cl]^+$ cation, namely that

Table 4. Relevant bond lengths (Å), angles (°), and τ values

(*a*) [Cu(bipy)$_2$Cl]Y cation distortion isomers

	Y = OH·6H$_2$O (**1**)[9]	Cl·6H$_2$O (**2**)[a]	PF$_6$·H$_2$O (**3**)[10]	NO$_3$·3H$_2$O (**4**)[4]	½(S$_5$O$_6$·6H$_2$O) (**5**)[b]
Cu–N(1)	1.983	1.989	1.996	1.989	1.992
Cu–N(2)	2.080	2.077	2.105	2.089	2.092
Cu–N(3)	1.994	1.970	2.005	1.989	1.988
Cu–N(4)	2.088	2.087	2.108	2.112	2.106
Cu–Cl	2.374	2.361	2.344	2.308	2.292
$\Delta N_{2,4}$	0.008	0.010	0.003	0.023	0.014
α_1 N(2)–Cu–Cl	118.7	118.7	115.7	127.8	130.7
α_2 N(4)–Cu–Cl	118.7	118.6	120.5	123.4	122.0
α_3 N(2)–Cu–N(4)	122.6	122.0	123.8	108.8	107.3
α_4 N(1)–Cu–Cl	89.7	90.9	92.2	93.1	92.0
α_5 N(3)–Cu–Cl	91.5	90.9	92.1	92.0	93.3
α_6 N(1)–Cu–N(2)	80.2	79.3	79.6	75.9	79.9
α_7 N(3)–Cu–N(4)	80.1	79.8	80.1	80.0	79.7
α_8 N(1)–Cu–N(3)	178.7	178.3	175.5	174.9	174.0
α_9 N(2)–Cu–N(4)	99.6	99.3	99.0	97.6	96.7
α_{10} N(1)–Cu–N(4)	98.9	100.0	96.4	96.6	97.5
τ value	1.00	1.00	1.00	0.79	0.74

	Y = Cu^{I}Cl$_2$ (**6**)[c]	BF$_4$ (**7**)	ClO$_4$ (**8**)[4]	(NC)$_2$C(CN)C(CN)$_2$ (**9**)[11]
Cu–N(1)	1.985	2.006	1.993	1.969
Cu–N(2)	2.063	2.079	2.076	2.062
Cu–N(3)	1.995	1.983	1.991	1.998
Cu–N(4)	2.086	2.142	2.136	2.118
Cu–Cl	2.356	2.285	2.263	2.277
$\Delta N_{2,4}$	0.023	0.063	0.059	0.056
α_1 N(2)–Cu–Cl	133.4	134.8	137.1	138.5
α_2 N(4)–Cu–Cl	111.1	127.6	126.4	114.2
α_3 N(2)–Cu–N(4)	115.5	97.6	96.5	107.3
α_4 N(1)–Cu–Cl	91.0	93.1	93.4	93.6
α_5 N(3)–Cu–Cl	93.5	91.7	92.1	92.0
α_6 N(1)–Cu–N(2)	80.0	79.9	80.1	80.3
α_7 N(3)–Cu–N(4)	80.2	79.5	79.2	78.6
α_8 N(1)–Cu–N(3)	175.3	175.2	174.5	174.3
α_9 N(2)–Cu–N(4)	97.0	97.8	96.0	97.9
$\alpha_1{}^0$ N(1)–Cu–N(4)	97.0	96.7	97.4	96.4
τ value	0.70	0.67	0.62	0.60

	(*b*) [Cu(bipy)$_2$Br]Y		(*c*) [Cu(bipy)$_2$I]Y	
	Y = Br (**10**)[27]	BF$_4$ (**11**)[28]	I (**12**)[29]	ClO$_4$ (**13**)[28]
Cu–N(1)	1.977	1.996	1.988	1.989
Cu–N(2)	2.075	2.068	1.961	2.090
Cu–N(3)	1.978	1.995	2.021	1.987
Cu–N(4)	2.085	2.114	2.106	2.100
Cu–Cl	2.429	2.419	2.697	2.675
$\Delta N_{2,4}$	0.010	0.046	0.145	0.010
α_1 N(2)–Cu–Cl	128.6	134.5	121.9	122.9
α_2 N(4)–Cu–Cl	124.7	126.2	124.4	122.8
α_3 N(2)–Cu–N(4)	106.7	99.4	113.8	114.3
α_4 N(1)–Cu–Cl	90	93.0	89.1	93.8
α_5 N(3)–Cu–Cl	91.4	91.2	91.5	91.0
α_6 N(1)–Cu–N(2)	80.4	80.1	81.2	80.3
α_7 N(3)–Cu–N(4)	80.3	79.6	83.1	80.1
α_8 N(1)–Cu–N(3)	177.3	175.6	175.9	174.4
α_9 N(2)–Cu–N(4)	96.9	97.0	99.9	94.9
$\alpha_1{}^0$ N(1)–Cu–N(4)	100.3	97.7	95.03	99.5
τ value	0.81	0.69	0.90	0.86

[a] F. S. Stephens and P. A. Tucker, *J. Chem. Soc., Dalton Trans.*, 1973, 2293. [b] W. D. Harrison, B. J. Hathaway, and D. Kennedy, *Acta Crystallogr., Sect. B*, 1979, **35**, 2301. [c] J. Kaiser, G. Brauer, F. A. Schroeder, I. F. Taylor, and S. E. Rasmussen, *J. Chem. Soc., Dalton Trans.*, 1974, 1490.

Table 5. Single-crystal or polycrystalline e.s.r. and electronic reflectance spectral data for $[Cu(bipy)_2Cl]Y$ complexes

Y	Single-crystal e.s.r.			Electronic reflectance peak maxima (10^3 cm^{-1})	
(1) $OH{\cdot}6H_2O$	—	—	—	—	—
(2) $Cl{\cdot}6H_2O$	2.085	2.180	2.094	12.5	—
(3) $PF_6{\cdot}H_2O$	2.029	2.203	2.216	12.0	—
(4) $NO_3{\cdot}3H_2O$	1.998	2.140	2.210	13.5	11.5
(5) $\frac{1}{2}(S_5O_6{\cdot}6H_2O)$	2.014	2.100	2.210	13.2	10.4
(6) Cu^ICl_2	2.049	2.201*	—	12.5	10.1
(7) BF_4	2.01	2.20*	—	13.9	10.1
(8) ClO_4	2.007	2.125	2.234	14.2	10.1
(9) $(NC)_2C(CN)(CN)_2$	—	—	—	—	—

* Polycrystalline e.s.r.

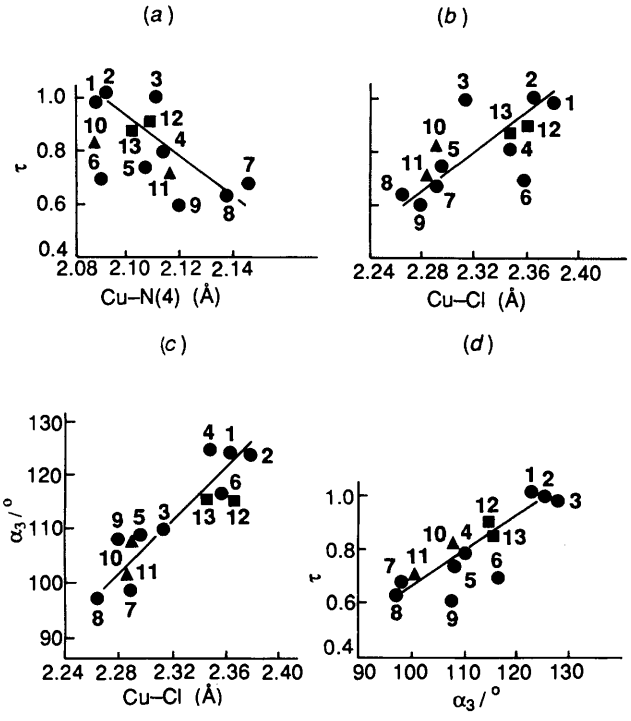

Figure 5. Four scatter plots for the $[Cu(bipy)_2X]Y$ complexes, including the τ value: X = Cl (●), Br (▲), or I (■). (*a*) τ *vs.* Cu–N(4), (*b*) τ *vs.* Cu–Cl, (*c*) α_3 *vs.* Cu–Cl, and (*d*) τ *vs.* α_3

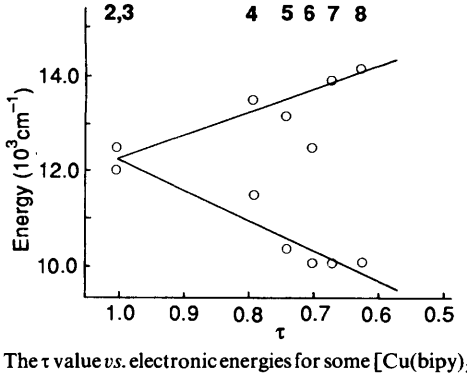

Figure 6. The τ value *vs.* electronic energies for some $[Cu(bipy)_2X]Y$ complexes

with decreasing τ value (*a*) the Cu–N(4) distance and the α_1 angle increase and (*b*) the Cu–Cl and Cu–N(2) distances and the α_2 and α_3 angles decrease, as originally suggested.[4] They also show that the τ values only vary in the range 1.0—0.6, reflecting the limited extent of the square-based pyramidal distortion of the trigonal-bipyramidal stereochemistry of the $[Cu(bipy)_2Cl]^+$ cation. In general the scatter plots justify the conclusions of ref. 4, that the individual structures of the $[Cu(bipy)_2Cl]^+$ cation represent the individual points along a continuous structural pathway, from a near regular trigonal-bipyramidal CuN_4Cl chromophore (τ = 1.0) towards a square-based-pyramidal distorted trigonal-bipyramidal CuN_4Cl chromophore (τ = 0.6).

In addition to the nine sets of data in Table 4, crystallographic data sets are available for two $[Cu(bipy)_2Br]^+$ cations[27,28] and two $[Cu(bipy)_2I]^+$ cations,[28,29] molecular structures (**10**)—(**13**). If the Cu–X distances for these four structures are corrected to correspond to the Cu–Cl distance,[14] by subtracting 0.14 and 0.33 Å, respectively, the bond length and angle data can be added to Figure 5. The correlation is actually improved in only one case, four are not significantly different, and six are reduced, notwithstanding the increase from 9 to 13 data sets. This suggests that the addition of the four data sets for the bromide and iodide to the nine data sets for the chloride is not justified. Nevertheless, from the visual appearance of the plots the data for the bromo and iodo complexes do show a reasonable correlation with the chloro scatter plots. This suggests that the former complexes may lie on a structural pathway that lies very close to that of the chloro series, the establishment of which must await the determination of additional bromo and iodo crystal structures.

The earlier reference to the use of scatter plots for $[Cu(bipy)_2Cl]Y$ complexes[4] also suggested an 'electronic criteria of stereochemistry,' based on the change from a single peak in the electronic spectrum of a near-trigonal-bipyramidal complex (τ = 1.0) to two peaks for the square-based-pyramidal distorted trigonal-bipyramidal complex (τ = 0.60) with a ΔE of *ca.* 4 000 cm^{-1}. The currently available scatter plot data are shown in Figure 6 and clearly suggest that ΔE increases with decreasing τ value.

Factor Analysis.—The advantage of the scatter plots shown is that they give a visual display of the crystallographic data, their ranges, and their variations. Unfortunately, they do not quantify these variations, although the τ values were a partial move in this direction. If the progress down the structural pathway is primarily due to two major factors, the *e'* modes of Figure 1, it would be attractive if a quantitative measure of the factors for the A and B (or C) routes were available, and also a measure of their relative contribution. Such information can be obtained by the application of factor analysis[12] to the data of Table 4. To do this the program FACAN[13] has been used (*a*) to characterise the major factors that contribute to the structural pathway and (*b*) to estimate their relative contribution, namely, their eigenvectors.

The FACAN program is a statistical package that ideally

requires extensive data. It has been used to examine the structural pathway of Figure 1, by taking 26 crystallographic data sets of CuN_4X chromophore containing $[Cu(L–L)_2X]Y$ complexes, where L–L = bipy or phen (1,10-phenanthroline) nitrogen chelate ligands and X = Cl, Br, I, O, N, or S type monodentate ligands.[14] This analysis included six of the complexes of Table 4, and came to similar conclusions to that of ref. 4. However, this procedure makes two assumptions concerning the 26 complexes: first, no distinction was made between whether the complexes involved the A or B (or C) type distortion routes, and secondly, *no distinction* was made between the types of chelate nitrogen ligands or between the donor X ligands. In the latter case, the different covalent radii of the donor atoms were corrected for, but for the carboxylate ligands, X, no account was taken of the bite angle[30,31] of these ligands, nor that these types of complexes are well known to involve fluxional type stereochemistries.[3,32,33] For these reasons the present paper has taken a more cautious approach, initially, using only one type of chelate ligand, bipy, and only one type of ligand X, Cl^-, and only then exploring the inclusion of the Br^- and I^- anions, with suitable correction of the Cu–X distances. By looking, initially, at only a single series of cation distortion isomers, it is hoped to determine whether the observed stereochemistry of the CuN_4X chromophore is sensitive to the type of chelate ligand and the nature of the X ligand. For this reason the initial FACAN analysis was limited to the nine structures of Table 4(*a*), thus restricting the analysis to the B and C route distortions of Figure 1, and which are related by the C_2 symmetry axis.

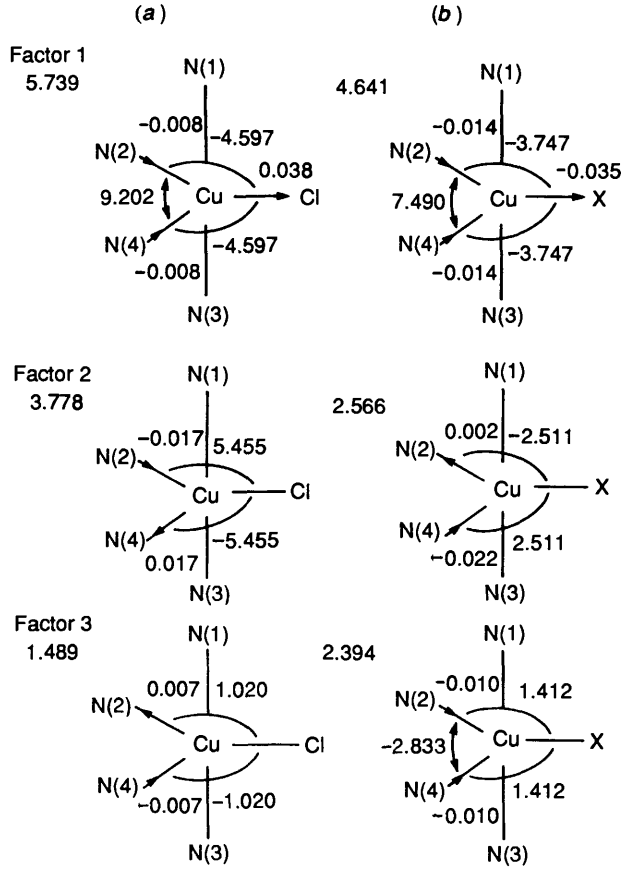

Figure 7. The highest deformation factors 1—3, for (*a*) $[Cu(bipy)_2Cl]Y$ and (*b*) $[Cu(bipy)_2X]Y$; X = Cl, Br or I

Figure 7(*a*) shows the three highest deformation factors obtained for the nine chloride data sets, and Figure 7(*b*) the corresponding factors with the inclusion of the two bromide and two iodide structures, a total of 13 data sets. In both cases the highest deformation factor, 1, corresponds to a symmetric mode of distortion, the Cu–X distance increasing with increasing α_3 angle. The next highest deformation, factor 2, corresponds to an asymmetric mode of distortion, with the Cu–N(2) distance decreasing, the Cu–N(4) distance increasing, the α_1 angle increasing, and the α_2 angle decreasing. The third deformation factor, 3, for the chloride series, Figure 7(*a*), features a comparable angular distortion to factor 2, but with the bond-length displacements reversed and reduced in significance. In any case, Figure 7(*a*), the significance of factor 3 is sufficiently low, 1.49, that it is not considered statistically significant. For Figure 7(*b*) factor 3 is more significant, but is also essentially a negative factor 1. Thus the two main factors for both series of Figure 7(*a*) and (*b*) correspond with each other and also to the two symmetric and asymmetric vibrational modes of distortion[4] of Figure 1.

In Figure 8 the geometries of the CuN_4X chromophores are projected onto the two main deformation factors, 1 and 2. Because of the C_2 axis relationship connecting the B and C routes of distortion the C_2 axis of symmetry is still retained. In the case of the chloride complexes alone, Figure 8(*a*), factor 1 contributes to the main spread of the points, with only a small contribution from factor 2. If the points for the two exceptional

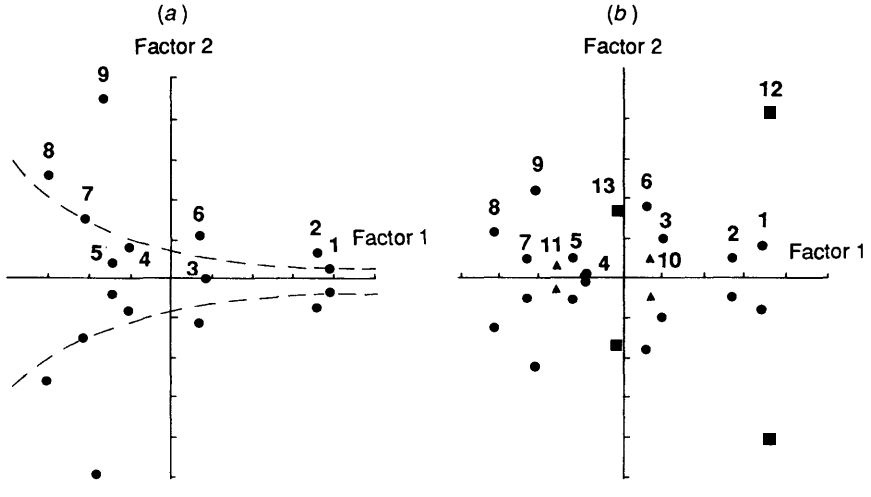

Figure 8. Projections of the $[Cu(bipy)_2X]Y$ geometry onto the two main factors, 1 and 2; X = Cl (●), Br (▲), or I (■)

structures, (**6**) and (**9**), are removed, see earlier, the points for the remaining seven complexes lie along a reasonable bifurcated curve (– – –), as suggested from the earlier FACAN analysis[14] of the 26 data sets. In the plot of Figure 8(*b*) factor 1 still makes the most significant contribution, but the contribution of factor 2 is more significant and the two iodide points lie well off the bifurcated curves of Figure 8(*a*). This suggests that two bromide complexes,[27,28] do show a reasonable correlation with the chloride data alone, that they do lie along a comparable structural pathway to that of the chloride, and that there is some justification in including the bromide data with the original chloride data, for the purpose of the FACAN analysis. The two iodide structures[29,30] [Figure 8(*b*)] clearly show that there is no correlation with the chloride data and that these complexes should not be included for the purpose of the FACAN analysis. However, caution is expressed over both of these suggestions, as they are based on only two bromide and two iodide structures, with one of the latter a very early structure determination.[29] Thus, until more structures are available, the above should be treated as tentative suggestions.

Acknowledgements

The authors acknowledge the award of Senior Studentships (to P. N. and E. O'S.), data collection by Dr. M. McPartlin and Mr. A. Bashall (Department of Applied Chemistry and Life Sciences, Polytechnic of North London), the Computer Bureau, University College Cork (U.C.C.), for computing facilities, Professor G. M. Sheldrick, Drs. P. Roberts, S. Motherwell, K. Henrick, and K. Davies, for the use of their programs, and the Microanalysis Section, U.C.C., for analysis.

References

1 H. A. Jahn and E. Teller, *Proc. R. Soc. London*, 1937, **161**, 220.
2 J. Gazo, I. B. Bersuker, J. Garaj, M. Kabesova, J. Kohout, H. Langfeldora, M. Melnick, M. Serator, and F. Valach, *Coord. Chem. Rev.*, 1976, **21**, 253.
3 B. J. Hathaway, *Struct. Bonding (Berlin)*, 1984, **57**, 55.
4 W. D. Harrison, D. M. Kennedy, N. J. Ray, R. Sheahan, and B. J. Hathaway, *J. Chem. Soc., Dalton Trans.*, 1981, 1556.
5 L. Hullet, R. Sheahan, N. Ray, and B. J. Hathaway, *J. Inorg. Nucl. Chem. Lett.*, 1978, **14**, 305.
6 R. L. Harlow, W. J. Wells, G. W. Watt, and S. H. Simonsen, *Inorg. Chem.*, 1975, **14**, 1468.
7 D. Reinen and C. Friebel, *Struct. Bonding (Berlin)*, 1979, **37**, 1.
8 K. L. Bray and H. G. Drickamer, *J. Phys. Chem.*, 1989, **93**, 7604; personal communication, 1990.
9 S. G. Teoh, H. K. Fun, and B. T. Chan, *J. Fizik Mal.*, 1987, **8**, 44.
10 S. Tyagi, B. J. Hathaway, S. Kremer, H. Stratemer, and D. Reinen, *J. Chem. Soc., Dalton Trans.*, 1984, 2087.
11 W. P. Jensen and R. A. Jacobson, *Inorg. Chim. Acta*, 1981, **50**, 189.
12 E. R. Malinowski and D. G. Howery, 'Factor Analysis in Chemistry,' Wiley, New York, 1980.
13 E. Muller, FACAN, program for factor analysis, written in Turbo Pascal (IBM and compatibles).
14 E. Muller, C. Piguet, G. Bernardinelli, and A. F. Williams, *Inorg. Chem.*, 1988, **27**, 849.
15 A. A. Scholt and R. C. Taylor, *J. Inorg. Nucl. Chem.*, 1959, **9**, 211.
16 L-P. Wu, Ph.D. Thesis, National University of Ireland, 1988.
17 F. S. Stephens, *J. Chem. Soc., Dalton Trans.*, 1972, 1350.
18 G. M. Sheldrick, SHELX 76, program for *X*-ray crystal structure determination, University of Cambridge, 1976.
19 G. M. Sheldrick, SHELX 86, program for *X*-ray crystal structure solutions, University of Göttingen, 1986.
20 D. T. Cromer and J. T. Waber, 'International Tables of Crystallography,' Birmingham, Kynoch Press, 1974, vol. 4, pp. 71, 148 (present distributor, Kluwer Academic Publishers, Dordrecht).
21 P. Roberts and G. M. Sheldrick, XANADU, program for the calculation of crystallographic data, University of Cambridge, 1979.
22 E. K. Davis, CHEM-X, molecular graphics program, currently developed and distributed by Chemical Design Ltd., Oxford, 1980.
23 K. Henrick, PUBTAB, program to prepare and print crystallographic tables for publication, 1980.
24 F. Huq and A. C. Shapski, *J. Chem. Soc. A*, 1971, 1927.
25 A. W. Addison, T. Nageswara Rao, J. Reedjik, J. van Rijn, and G. C. Verschoor, *J. Chem. Soc., Dalton Trans.*, 1984, 1349.
26 B. J. Hathaway, 'Comprehensive Coordination Chemistry. The Synthesis, Reactions, Properties and Applications of Coordination Compounds,' eds. G. Wilkinson, R. D. Gillard, and J. A. McCleverty, Pergamon, Oxford, 1988, vol. 5, sect. 53, p. 533.
27 M. A. Khan and D. G. Tuck, *Acta Crystallogr., Sect. B*, 1981, **37**, 1409.
28 B. J. Hathaway and A. Murphy, *Acta Crystallogr., Sect. B*, 1980, **36**, 295.
29 G. A. Barclay, B. F. Hoskins, and C. H. L. Kennard, *J. Chem. Soc.*, 1963, 5691.
30 N. Ray, S. Tyagi, and B. J. Hathaway, *Acta Crystallogr., Sect. B*, 1982, **38**, 1574.
31 B. J. Hathaway, 'Comprehensive Coordination Chemistry. The Synthesis, Reactions, Properties and Applications of Coordination Compounds,' eds. G. Wilkinson, R. D. Gillard, and J. A. McCleverty, Pergamon, Oxford, 1988, vol. 2, sect. 15.5, p. 413.
32 B. J. Hathaway, M. Duggan, A. Murphy, J. Mullane, C. Power, A. Walsh, and B. Walsh, *Coord. Chem. Rev.*, 1981, **36**, 267.
33 Ref. 31, p. 690.

Received 21*st May* 1990; *Paper* 0/02239J